Chapter 12 | Evaporation from Homogeneous Surfaces

12.1 The Process of Evaporation

The evaporation in the atmosphere and consequent phenomena of condensation, cloud formation, and precipitation have fascinated scientists, philosophers, and common people since time immemorial. Early philosophers and scientists proposed many theories and explanations of the evaporation process; for a brief review of the history the reader may refer to Brutsaert (1982). As early as the fourth century BC, Aristotle recognized that 'wind is more influential in evaporation than the sun.' However, it was not until the nineteenth century that the foundations of the modern quantitative theories of evaporation and other transport phenomena were laid by J. Dalton, A. Fick, and O. Reynolds.

Evaporation is the phenomenon by which a substance is converted from the liquid state into vapor state. In the atmospheric surface layer evaporation may take place from a free water surface or a moist soil surface, as well as from the leaves of living plants and trees (here, we are ignoring the distinction between evaporation and transpiration). The details of the physical process of conversion from the liquid to vapor state may differ in different cases, but the basic mechanisms of transport of vapor away from any interface are the same. Very close to the interface, vapor is transferred through molecular exchanges in the same manner as heat and momentum are transferred. Most of the transfer takes place within a few molecular free path lengths of the surface. The vigorous molecular activity in this region is indicated by the observation that an estimated 2 to 3 kg of water moves across a free water interface in each direction every second, for each square meter of the interface (Munn, 1966, Chapter 10). However, the net transport of water vapor is only a tiny fraction of the total transport in each direction. According to Fick's law, the net flux of a material (e.g., water vapor) in a given direction is proportional to its concentration (specific humidity) gradient in that direction, the coefficient of proportionality being defined as the molecular diffusivity. Thus, the evaporation rate at a horizontal surface is given by

$$E_0 = -\rho\alpha_w(\partial Q/\partial z) \tag{12.1}$$

in which α_w is the molecular diffusivity of water vapor. The above relationship is expected to be valid only in the laminar or viscous sublayer in which the molecular exchange remains the primary (perhaps the only) transport mechanism. The same mechanism is operating at the air–soil and air–leaf interfaces. However, natural surfaces, not being very smooth and uniform, may not have well-defined molecular sublayers which could be amenable to direct measurements. Therefore, the practical utility of Equation (12.1) for estimating evaporation in the atmosphere remains questionable. Some attempts have been made by physical chemists and fluid dynamists to study evaporation and the other transport processes on the molecular scale. Micrometeorologists are more interested, however, in turbulent exchange processes over the much larger scales that are encountered in the atmospheric surface layer and the PBL.

In the lower part (surface layer) of the atmospheric boundary layer the air motion is almost always turbulent. Here, the water vapor is efficiently transported away from the interfacial molecular sublayer by turbulent eddies. Because eddy transport and the intensity of turbulent mixing depend on the surface roughness, wind shear or friction velocity, and thermal stratification, the evaporation rate also depends on the above factors, as well as on the average specific humidity gradient. The frequently used gradient-transport relation for the same is

$$E = -\rho K_w(\partial Q/\partial z) \tag{12.2}$$

in which the eddy diffusivity K_w replaces the molecular diffusivity in Equation (12.1).

While Fick's law or Equation (12.1) has a firm theoretical (e.g., the kinetic theory of gases) and experimental basis, the analogous relation [Equation (12.2)] for a turbulent flow is based on a phenomenological gradient-transport theory whose limitations have already been pointed out in Chapter 9. Better flux-gradient relations obtained on the basis of the Monin–Obukhov similarity theory and carefully conducted micrometeorological experiments will be discussed in a later section.

12.2 Potential Evaporation and Evapotranspiration

Over a bare land surface with no standing water, the soil moisture is the only source of water for evaporation. Therefore, the rate of evaporation must depend on the moisture content of the topmost layer of the soil. When the soil surface is fully saturated and the soil moisture content is not a limiting factor in evaporation, this maximum rate of evaporation for the given surface weather conditions is called potential evaporation (E_p). When the soil becomes drier, the

rate of evaporation for the given atmospheric conditions (particularly the surface temperature, near-surface wind speed, specific humidity, and stability) also depends on the moisture content of the topmost soil layer which, in turn, depends on the soil moisture flow through the soil. The relationship between the rate of evaporation (E_0) and the soil moisture flow rate (M) is given by the instantaneous water balance equation at the surface

$$E_0 = M_0 \tag{12.3}$$

or the water balance equation for the subsurface layer,

$$E_0 = M_b - \Delta M \tag{12.4}$$

in which ΔM is the rate of storage of soil moisture in the layer per unit area of the surface, and M_b is the moisture flow rate at the bottom of the layer. The above simplified water budget equations would be valid only during the periods of no precipitation, irrigation, or runoff at the surface.

The vertical moisture flow rate, or the flux of soil moisture, is related to the vertical gradient of the soil moisture content (S) through Darcy's law

$$M = -k_m(\partial S/\partial z) \tag{12.5}$$

where k_m is the hydraulic conductivity through the soil medium. Note that Equation (12.5) (Darcy's law) is analogous to Equation (4.1) (Fourier's law) for heat conduction. Similarly, following the derivation of Fourier's heat conduction equation [Equation (4.2) or (4.3)], one can obtain

$$(\partial/\partial t)(\rho S) = -\partial M/\partial z \tag{12.6}$$

or, after substituting from Equation (12.5),

$$\partial S/\partial t = (\partial/\partial z)[\alpha_m(\partial S/\partial z)] \tag{12.7}$$

where $\alpha_m = k_m/\rho$ is the diffusivity of soil moisture.

For surfaces with live vegetation, a significant portion of water vapor transfer to the atmosphere is by transpiration from the vegetation, most of which takes place through the stomata of leaves. Transpiration may be considered an important by-product of the process of photosynthesis and respiration, in which plants take CO_2 during daytime and give out the same at nighttime. Transpiration may also be a physiological necessity for plants to draw up dissolved nutrients from the soil through their roots. Moisture transfer through roots, stands, and leaves is considerably more efficient than

that through the soil pores, because the former is forced by a strong osmotic pressure gradient. Still, evaporation from the bare soil surface in between the plants is by no means negligible. Because evaporation and transpiration occur simultaneously and it is not easy to distinguish between the vapor transferred by the two processes, the term evapotranspiration is sometimes used to describe the total water vapor transfer to the atmosphere. More often, though, meteorologists use evaporation as a substitute or synonym for evapotranspiration. The distinction between the two disappears, anyway, when one considers the vegetative surface as a composite of soil and leaf surfaces, which contribute to the total water vapor transfer (evaporation) to the atmosphere per unit horizontal area of the composite surface, per unit time. In this gross sense, details of the vegetation canopy (e.g., leaves and branches) and small-scale transfer processes around the individual surface elements are essentially glossed over and the canopy is considered as an idealized, homogeneous material layer which has a finite thickness and mass, and which can store or release heat and water vapor. In particular, the detailed water budget for a vegetative surface is often too complicated to be used as a practical tool for estimating evaporation.

The concept of potential evaporation (E_p) can also be extended to any vegetative surface for which E_p represents the maximum evapotranspiration likely from the vegetative surface for a given set of surface weather conditions. The potential evapotranspiration is generally less than the free water surface evaporation under the same weather conditions, especially in humid regions. The former can exceed the latter, however, in certain arid regions and under certain weather conditions (Rosenberg *et al.*, 1983, Chapter 7).

Actual evaporation usually differs from the potential evaporation, because the surface may not be saturated and the plants may not be drawing water from the soil and transpiring at their maximum rate. Still, the concept of potential evaporation is quite useful in agricultural and hydrological applications.

12.3 Modified Monin–Obukhov Similarity Relations

The original Monin–Obukhov similarity hypothesis and subsequent relations based on the same, as discussed in the preceding chapter, are strictly valid when buoyancy effects of water vapor can be ignored. When substantial evaporation occurs and it affects the density stratification in the surface layer, modified M–O similarity relations incorporating the buoyancy effects of water vapor would be more appropriate.

Some buoyancy effects of water vapor have already been discussed in Chapter 5, where the concepts of virtual temperature and virtual potential temperature were introduced. A similar concept is that of the virtual heat flux H_v, which may

be interpreted as the flux of virtual temperature ($H_v = \rho c_p \overline{w\theta_v}$). The modified Monin–Obukhov similarity hypothesis states that, in a homogeneous and stationary atmospheric surface layer, the mean gradients and turbulence structure depend only on four independent variables: z, u_*, g/T_{v0}, and $H_{v0}/\rho c_p$. As mentioned in Chapter 5, the difference between the virtual temperature and actual temperature is no more than 7 K and frequently less than 2 K, so that the buoyancy parameter g/T_{v0} does not differ much from g/T_0. However, the virtual heat flux may differ significantly from the actual heat flux, and the two are approximately related as

$$H_v \cong H + 0.61 c_p \Theta E \tag{12.8}$$

This follows from the approximate relationship between the fluctuations of virtual temperature, actual temperature, and specific humidity

$$\theta_v \cong \theta + 0.61 \Theta q \tag{12.9}$$

which, in turn, can be derived from the relationship between $\tilde{\Theta}_v$ and $\tilde{\Theta}$, noting that $\tilde{\Theta}_v = \Theta_v + \theta_v$ and $\tilde{\Theta} = \Theta + \theta$. These derivations are left as an exercise for the reader.

The relation given by Equation (12.8) can also be expressed in terms of the latent heat flux H_L, or the Bowen ratio B, as

$$H_v = \mathrm{H} + \alpha_\theta H_L = H(1 + \alpha_\theta B^{-1}) \tag{12.10}$$

in which $\alpha_\theta = 0.61 c_p \Theta / L_e$ is a dimensionless coefficient. Since α_θ is only weakly dependent on the absolute temperature, a constant value of $\alpha_\theta = 0.07$, corresponding to $\Theta = 280$ K, is frequently used in the above relations. From Equation (12.10) it is obvious that the suggested modification to the M–O hypothesis is necessary only when $|B| < 1$, i.e., when the latent heat flux exceeds the sensible heat flux. This is usually the case over the oceans, but not so common over the land areas.

Note that in the modified similarity hypothesis both the sensible heat flux and water vapor flux are considered together in an appropriate combination (the virtual heat flux) and not separately. Therefore, a modified Obukhov length is defined as

$$L = -u_*^3 \Big/ \left(k \frac{g}{T_{v0}} \frac{H_{v0}}{\rho c_p} \right) \tag{12.11}$$

However, the scales of temperature, virtual temperature, and specific humidity have to be defined from their respective fluxes, i.e.,

$$\begin{aligned} \theta_* &= -H_0/(\rho c_p u_*) \\ \theta_{v*} &= -H_{v0}/(\rho c_p u_*) \\ q_* &= -E_0/(\rho u_*) \end{aligned} \tag{12.12}$$

The corresponding flux-profile relations for the transfer of water vapor in the atmospheric surface layer are

$$\begin{aligned} \frac{kz}{q_*}\frac{\partial Q}{\partial z} &= \phi_w\left(\frac{z}{L}\right) \\ \frac{Q - Q_0}{q_*} &= \frac{1}{k}\left[\ln\frac{z}{z_0} - \psi_w\left(\frac{z}{L}\right)\right] \\ E_0 &= -\rho C_W U(Q - Q_0) \end{aligned} \tag{12.13}$$

which are analogous to the heat transfer relations discussed in Chapter 11. Thus, the transfer of water vapor and other gaseous substances from the surface to the atmosphere or vice versa can be treated in the same way as the transfer of heat. The similarity between water vapor and heat transfer implies that

$$\begin{gathered} \phi_w(z/L) = \phi_h(z/L); \quad \psi_w(z/L) = \psi_h(z/L) \\ K_w = K_h; \quad C_W = C_H \end{gathered} \tag{12.14}$$

Experimental verification of Equations (12.14) has been done in a few micrometeorological studies. For example, simultaneous determinations of $\phi_h(z/L)$ and $\phi_w(z/L)$ from micrometeorological observations at Kerang, Australia, are compared in Figure 12.1. Note that there is no systematic and significant difference between these two functions, although there is more scatter in the estimates of $\phi_w(z/L)$, probably due to larger uncertainties in the eddy correlation measurements of $\overline{wq}$ as compared to $\overline{w\theta}$. Both of the empirical functions are well represented by the simpler Businger–Dyer relations [Equation (11.9)]. There is also some observational evidence for the equality of K_h and K_w under stable conditions (Oke, 1970; Webb, 1970). A number of air–sea interaction studies in the marine atmospheric surface layer have also confirmed the approximate equality of eddy diffusivities, as well as bulk transfer coefficients of heat and water vapor, especially in the absence of such complicating factors as breaking waves and water spray.

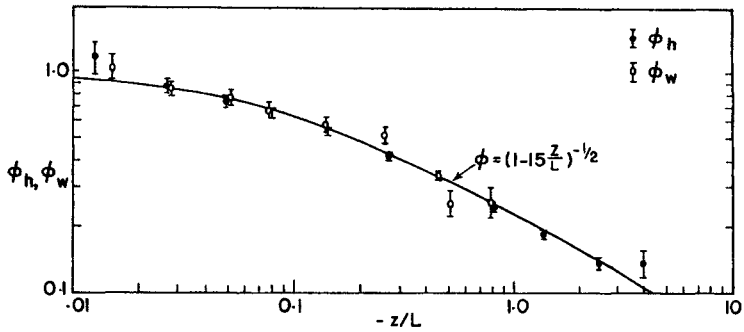

Figure 12.1 Comparison of the observed dimensionless potential temperature and specific humidity similarity functions for unstable conditions. [After Dyer (1967).]

There may be some exceptions to the above-mentioned similarity between heat and water vapor transfers and the implied equality of their eddy exchange coefficients and M–O similarity functions. For example, micrometeorological measurements made over irrigated fields under conditions of warm air advection, when heat and water vapor are transferred in opposite directions (e.g., downward sensible heat flux and upward water vapor flux), have shown K_h values to be generally larger than K_w (Verma *et al.*, 1978). Under such strong advection conditions, which are generally accompanied by strong winds and are representative of near-neutral or mild stability ($Ri < 0.01$), the ratio K_h/K_w is found to range between 1 and 3.

12.4 Micrometeorological Methods of Determining Evaporation

Depending on the application for which the rate of evaporation is to be estimated and the associated temporal and spatial scales, a large number of hydrological, climatological, and micrometeorological methods have been proposed in the literature for determining evaporation (Brutsaert, 1982, Chapters 8–11; Rosenberg *et al.*, 1983, Chapter 7; Garratt, 1992, Chapter 5). Here, we will restrict ourselves mainly to the micrometeorological methods which can be used to determine or measure the rate of evaporation at small time (order of an hour or less) and space (order of 1000 m or smaller) scales.

12.4.1 Direct measurements by lysimeters and evaporation pans

Instruments used for direct measurement of evaporation or potential evaporation from land surfaces are called lysimeters. A lysimeter is a cylindrical

container (1–2 m deep and 1–6 m in diameter) in which an undisturbed block of soil and vegetation is isolated and its water budget is carefully monitored and controlled. Changes in the mass of the lysimeter are monitored either by a sensitive balance (mechanical or electronic) installed underneath, or a manometer measuring differences of hydrostatic pressures. There are two types of lysimeters, namely, weighing and floating lysimeters. In the latter, representative samples are floated on liquids such as water, oil, or solutions of zinc chloride, and their weight changes are determined from the fluid displacements resulting from the changes in buoyancy of the floating sample. Precision lysimeters with accuracies of 0.01–0.02 mm equivalent of water evaporated are found to be most suitable for measuring evaporation on short time scales (less than an hour). The lysimeter dimensions depend on the type of vegetation on the surface and the depth of the root zone. An extreme example is that of a giant floating lysimeter containing a mature Douglas fir tree in a forest at Cedar River, Washington, which is used for measuring evapotranspiration from the tree (Oke, 1987).

Evaporation pans are used for measuring free water evaporation from small lakes and ponds. Many types of pans have been used over the years and some have been standardized. The diameters of cylindrical evaporation pans used in practice range from 1 to 5 m and their depths range from 0.25 to 1.0 m. Due to limitations of size and spurious edge effects, the evaporation rate from a pan is usually 5–30% larger than that from a small lake or a pond. Large, sunken pans are most representative of free water evaporation in the absence of breaking waves and spray.

Evaporation pans have also been used for estimating potential evapotranspiration E_p from vegetative surfaces. Since, evaporation from a pan depends on its size, location, and exposure to sun and winds, calibration of a pan against measured potential evapotranspiration may be necessary for this method to be reliable. The ratio of potential evapotranspiration to pan evaporation on time scales of 1–30 days has been found to vary between 0.5 and 1.5 (this range may be expected to be even larger for small time scales of interest in micrometeorology). It depends on the pan size and exposure, geographical location, weather conditions, season, and the type of vegetation and its growth stage.

Other inexpensive instruments for estimating potential evaporation are atmometers, which are essentially porous ceramic or paper evaporating surfaces. The evaporating surface is continuously supplied with water; the measured rate at which water must be supplied to keep the porous material saturated is a measure of potential evaporation for given weather conditions. Again, calibration against a standard instrument or technique is necessary for an atmometer to be useful.

12.4.2 Eddy correlation method

A direct method of measuring the local water vapor flux over a homogeneous or nonhomogeneous surface is to measure simultaneously turbulent velocity and specific humidity fluctuations and determine their covariance over the desired sampling or averaging time. It is based on the relationship

$$E = \rho \overline{wq} \tag{12.15}$$

where E is the vertical flux of water vapor. Over a homogeneous surface, if eddy correlation measurements are made in the constant flux surface layer, the rate of evaporation from the surface is also given by Equation (12.15), as $E \cong E_0$.

This method is simple in theory, but very difficult to use in practice, because the fast-response instruments required for measuring vertical velocity and specific humidity fluctuations need great care to install, maintain, calibrate, and operate. Reliable fast-response humidity instruments, such as the Lyman–Alpha humidiometer, microwave refractometer/hygrometer, and infrared hygrometer have been developed (Hay, 1980; Lenschow, 1986). Such sophisticated instruments and the eddy correlation method have so far been used only during certain research expeditions and not for routine measurements of evaporation.

12.4.3 Energy balance/Bowen ratio method

The energy budgets of various types of surfaces, as well as of interfacial layers, have been discussed in Chapter 1. As mentioned in Chapter 11, the appropriate energy budget equation can be used to determine the sum of sensible and latent heat fluxes from measurements or estimates of the rest of the budget terms. Further partitioning of this into sensible and latent heat fluxes can be done if their ratio $B = H/H_L$ is measured or can otherwise be estimated. Then, Equation (2.3) can be used to determine the latent heat flux H_L from which

$$E_0 = H_L/L_e \tag{12.16}$$

The Bowen ratio can be estimated from the gradient transport relations for H and E, with the assumption of the equality of the eddy exchange coefficients K_h and K_w. It is easy to show that

$$B = \frac{c_p}{L_e} \frac{\partial \Theta / \partial z}{\partial Q / \partial z} \cong \frac{c_p}{L_e} \frac{\Delta \Theta}{\Delta Q} \tag{12.17}$$

where $\Delta\Theta = \Theta_2 - \Theta_1$ and $\Delta Q = Q_2 - Q_1$. Thus, in order to determine B one needs to measure the differences in temperature and specific humidities at two levels in the surface layer. This can be easily done through the use of dry- and wet-bulb thermometers or thermocouples, preferably in a difference circuit.

Another method of estimating the Bowen ratio is discussed later in the context of the Penman approach.

12.4.4 Bulk transfer approach

This is similar to the bulk transfer method for determining the surface heat flux. The appropriate bulk transfer formula for the water vapor flux is

$$E_0 = \rho C_w U_r (Q_0 - Q_r) \tag{12.18}$$

in which Q_0 is the mean specific humidity very close to the surface (more appropriately, at $z = z_0$) and C_w is the bulk transfer coefficient for water vapor, which can be specified or parameterized in the same manner as C_H (Reynolds' analogy between water vapor and heat transfers implies $C_W = C_H$). This approach requires measurements of wind speed, temperature, and specific humidity at a reference height, a good estimate of the surface roughness z_0, and the temperature and specific humidity at z_0. The main difficulty is that Θ_0 and Q_0 are not easy to measure or estimate, especially for vegetative surfaces. For such surfaces the zero-plane displacement height d_0 must also be estimated, as Θ_0 and Q_0 refer to the height $d_0 + z_0$.

Alternative forms of the bulk-transfer relations that are frequently used to parameterize the surface fluxes of sensible heat and water vapor are

$$\begin{aligned} H_0 &= \rho c_p C_H U_r (\Theta_s - \Theta_r) \\ E_0 &= \rho C_W U_r (Q_s - Q_r) \end{aligned} \tag{12.19}$$

in which Θ_s and Q_s denote the potential temperature and specific humidity right at the surface. The use of Θ_s and Q_s is more appropriate if their values are readily available from observations or can be obtained from the prognostic equations for Θ_s and Q_s.

Over large lake, sea and ocean surfaces, the water surface temperature T_s is routinely available from satellite measurements. It has been estimated by bucket water temperature in most field experiments on air–sea interactions. Due to very small values of z_0 over water surfaces, no distinction is usually made between Θ_0 and Θ_s, or between Q_0 and Q_s. The specific humidity near the water surface is determined simply as the saturation value at T_s. An experimental verification of Equation (12.19) is given in Figures 12.2 and 12.3, in which vertical fluxes of

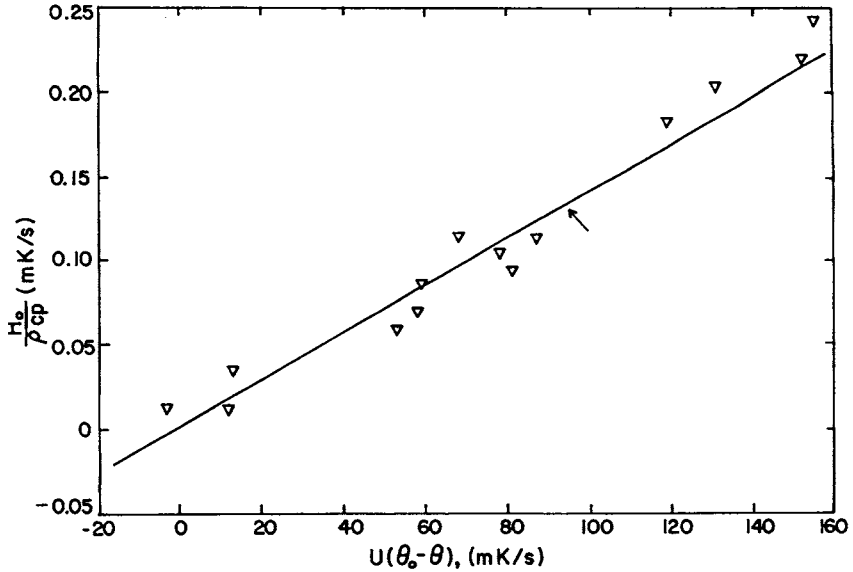

Figure 12.2 Sensible heat flux at the sea surface as a function of $U(\Theta_0 - \Theta)$ in strong winds compared with Equation (12.19) with $C_H = 1.14 \times 10^{-3}$. [After Friehe and Schmitt (1976); data from Smith and Banke (1975).]

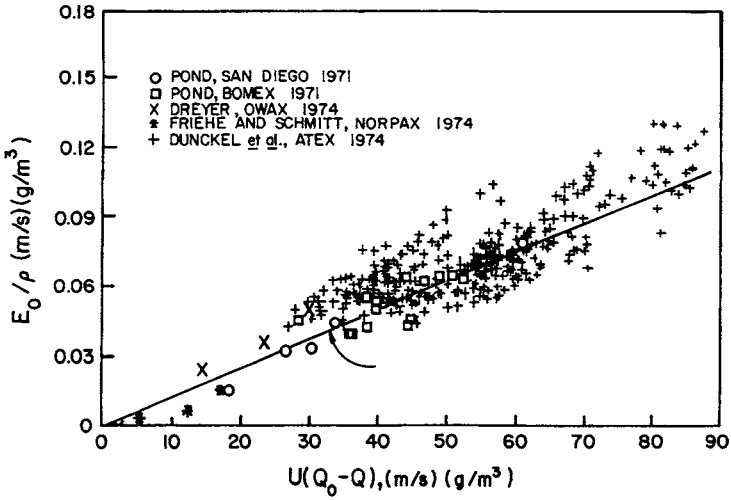

Figure 12.3 Observed moisture flux at the sea surface as a function of $U(Q_0 - Q)$ compared with Equation (12.18) with $C_W = 1.32 \times 10^{-3}$. [After Friehe and Schmitt (1976).]

heat and moisture are shown to be well correlated (nearly proportional) with the products $U_r(\Theta_s - \Theta_r)$ and $U_r(Q_s - Q_r)$, respectively, at a reference height $z_r = 10$ m. Note that the bulk transfer coefficients C_H and C_W are given by the slopes of the regression lines passing through the origin in Figures 12.2 and 12.3, respectively.

A central objective of many air–sea interaction experiments and expeditions has been the empirical determination of the drag, heat, and water vapor transfer coefficients (C_D, C_H, and C_W), covering a wide range of surface roughness, sea state, and stability conditions. Under moderate winds ($6 < U_{10} < 12 < \text{m s}^{-1}$) and near-neutral stability, there is an overwhelming experimental evidence indicating that $C_{DN} \cong C_{HN} \cong C_{WN} \cong 1.2 \times 10^{-3}$. Under more typical, slightly unstable conditions prevailing over the oceans, however, transfer coefficients are somewhat larger, but still approximately equal to each other ($C_D \cong C_H \cong C_W \cong 1.5 \times 10^{-3}$), at least within the estimated margin of error ($\pm 20\%$) of their determination (Pond, 1975). These results point to a rather simple parameterization of air–sea fluxes in terms of wind speed, temperature, and specific humidity at the 10 m level and the sea-surface temperature.

Atypical or exceptional stability conditions may be encountered, of course, over certain oceanic areas and during certain weather conditions when C_D, C_H, and C_W may differ considerably from their above typical values. For example, in the areas and periods of intense cold-air advection over the warmer ocean, free convection may occur in which C_H and C_W are expected to become considerably larger than $C_D > 1.5 \times 10^{-3}$. On the other hand, under inversion conditions and light winds, all the transfer coefficients are expected to become much smaller than their neutral value.

The stability effects on the drag and other transfer coefficients can be considered in the framework of the Monin–Obukhov similarity theory. For example, Equation (11.17) can be expressed in the form

$$\begin{aligned} C_D/C_{DN} &= [1 - k^{-1}C_{DN}^{1/2}\psi_m(z/L)]^{-2} \\ C_H/C_{DN} &= [1 - k^{-1}C_{DN}^{1/2}\psi_m(z/L)]^{-1}[1 - k^{-1}C_{DN}^{1/2}\psi_h(z/L)]^{-1} \end{aligned} \tag{12.20}$$

expressing the ratios C_D/C_{DN} and C_H/C_{DN} as functions of C_{DN} and z/L. These can also be expressed in terms of the more convenient bulk Richardson number $\text{Ri}_B = gz(\Theta_v - \Theta_{v0})/T_{v0}U^2$, using the following relations between z/L and Ri_B:

$$\begin{aligned} z/L &\cong kC_{DN}^{-1/2}\text{Ri}_B, && \text{for } \text{Ri}_B < 0 \\ z/L &\cong kC_{DN}^{-1/2}\text{Ri}_B(1 - 5\text{Ri}_B)^{-1} && \text{for } \text{Ri}_B \geq 0 \end{aligned} \tag{12.21}$$

The first of these relations is only an approximation to the more exact but implicit relationship between z/L and $\mathrm{Ri_B}$. The ψ functions in Equation (12.20) are given by Equation (11.14), so that the ratios C_D/C_{DN} and C_H/C_{DN} can be evaluated as functions of $\mathrm{Ri_B}$. Figure 12.4 shows that these are only weakly dependent on the neutral value of the drag coefficient (C_{DN}), but have rather strong dependence on $\mathrm{Ri_B}$, particularly in stable conditions.

Over land surfaces, Θ_s can be determined from the prognostic equation [Equation (4.14)] for the ground surface temperature T_s, in which the sensible and latent heat fluxes are expressed using the bulk-transfer relations (12.19). The surface specific humidity, Q_s, is usually estimated from T_s and wetness or moisture content of the surface, using a variety of simple, noninteractive, or more complicated, interactive schemes that have been proposed (Garratt, 1992, Chapter 8).

For a bare saturated soil surface, Q_s is simply equal to the saturated specific humidity Q_s^* at T_s, and can be determined from Equations (5.11)–(5.13) or a corresponding thermodynamic (e.g., e_s versus T) diagram. For unsaturated or drying soil surfaces and for vegetated canopies in particular, Q_s is not so easily determined. Approximate diagnostic relations for Q_s, based on an assumed Bowen ratio, the surface relative humidity, or the ratio of actual to potential evaporation are often used. Sometimes, interactive schemes utilizing the so-called 'bucket' and 'force restore' methods are employed (Garratt, 1992, Chapter 8).

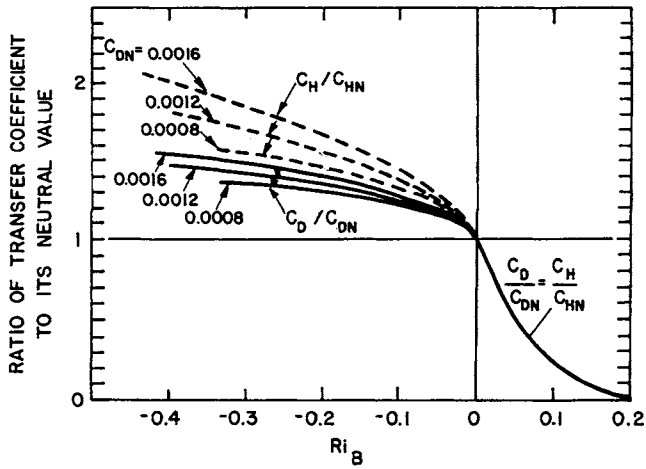

Figure 12.4 Calculated ratios of the drag and heat transfer coefficients to their neutral values as functions of the bulk Richardson number and C_{DN}. [After Deardorff (1968).]

The presence of a vegetation canopy makes the above bulk-transfer approach to flux parameterization very crude and somewhat dubious. The difficulty comes from our inability to define and determine the effective surface temperature and specific humidity without a detailed canopy model or parameterization. An introduction to canopy modeling and parameterization will be given later in Chapter 15.

Example Problem 1

The following meassurements were made on the research vessel FLIP during the 1969 Barbados Oceanographic and Meteorological Experiment (BOMEX):

Mean wind speed at 10.9 m above the sea surface = 7.96 m s^{-1}.
Mean temperature at 10.9 m = 27.34°C.
Mean specific humidity at 10.9 m = 16.04 g kg^{-1}.
Sea-surface temperature = 28.35°C.
Surface pressure = 1000 mbar.

Using the bulk-transfer relations with $C_D = C_H = C_W = 1.5 \times 10^{-3}$, calculate the surface stress, the sensible heat flux, and the rate of evaporation at the time of these observations. Also estimate the Bowen ratio and the virtual heat flux at the surface.

Solution

First, we calculate the saturation specific humidity Q_s corresponding to the observed sea-surface temperature $T_s = 301.50$ K. For this, we can use Equation (5.13) for determining the saturation water vapor pressure e_s as

$$\ln\frac{e_s}{6.11} = \frac{m_w L_e}{R_*}\left(\frac{1}{273.2} - \frac{1}{301.5}\right)$$

$$= \frac{18.02 \times 10^{-3} \times 2.43 \times 10^6 (0.00366 - 0.00332)}{8.314}$$

$$= 1.791$$

so that $e_s = 36.62$ mbar

Then, from Equation (5.11),

$$Q_s = 0.622\frac{e_s}{P} = 0.02278$$

Next, the density of moist air near the surface can be determined from the equation of state as

$$\rho = \frac{P}{RT_v}$$

where,

$$T_v = T(1 + 0.61Q) = 301.5(1 + 0.61 \times 0.0228) = 305.7 \text{ K}$$

Thus,

$$\rho = \frac{1000 \times 100}{287.04 \times 305.7} \cong 1.14 \text{ kg m}^{-3}$$

Finally, using the bulk-transfer relations (11.16) and (12.19), the surface stress and heat and water vapor fluxes can be estimated as follows:

$$\begin{aligned}
\tau_0 &= \rho C_D U_r^2 = 1.14 \times 1.5 \times 10^{-3} \times (7.96)^2 \cong 0.108 \text{ N m}^{-2} \\
H_0 &= \rho c_p C_H U_r(\Theta_s - \Theta_r) \\
&= 1.14 \times 1004 \times 1.5 \times 10^{-3} \times 7.96(301.50 - 300.49 - 0.0098 \times 10.9) \\
&= 12.3 \text{ W m}^{-2} \\
E_0 &= \rho C_E U_r(Q_s - Q_r) \\
&= 1.14 \times 1.5 \times 10^{-3} \times 7.96(0.02278 - 0.01604) \\
&\cong 9.17 \times 10^{-5} \text{ kg m}^{-2} \text{ s}^{-1}
\end{aligned}$$

The Bowen ratio can be determined as

$$B = \frac{H_0}{L_e E_0} = \frac{12.3}{2.45 \times 10^6 \times 9.17 \times 10^{-5}} \cong 0.055$$

which may be compared with an indirect estimate from Equation (12.17)

$$B = \frac{c_p}{L_e} \frac{\Delta\Theta}{\Delta Q} = \frac{1004(301.50 - 300.60)}{2.45 \times 10^6(0.02278 - 0.01604)} \cong 0.055$$

The virtual heat flux at the surface can be estimated from Equation (12.10) with $\alpha_\theta = 0.07$ as

$$H_{v0} = H_0(1 + 0.07B^{-1}) = 12.3(1 + 1.28) \cong 28.0 \text{ W m}^{-2}$$

12.4.5 Penman approach

Using a combination of the energy balance and bulk transfer formulas, Penman (1948) derived a formula for evaporation from open water and saturated land surfaces, which considerably simplifies the observational procedure. Penman's formula, either in the original or slightly modified form, is widely used for estimating potential evaporation or evapotranspiration, especially in hydrological and agricultural applications. A modern derivation of the formula is given in the following discussion.

Equation (12.18) can be written in the form

$$\begin{aligned} E_0 &= \rho C_W U_r (Q_0 - Q_r^*) + E_a \\ E_a &= \rho C_W U_r (Q_r^* - Q_r) \end{aligned} \tag{12.22}$$

where Q_r^* represents the specific humidity at the reference height if air were saturated there, and E_a can be interpreted as the drying power of air, because it is proportional to the difference between the saturation humidity and the actual specific humidity of air at the reference height z_r.

If the measurement height is low (say, a few meters), the bulk transfer relation for surface heat flux can be approximated as

$$H_0 = \rho c_p C_H U_r (T_0 - T_r) \tag{12.23}$$

From Equations (12.22) and (12.23), assuming $C_W = C_H$, we obtain

$$\frac{L_e E_0}{H_0} = \frac{L_e}{c_p} \left(\frac{Q_0 - Q_r^*}{T_0 - T_r} \right) + \frac{L_e E_a}{H_0}$$

or, after converting specific humidities into water vapor pressures through Equation (5.11),

$$B^{-1} = \frac{0.622 L_e}{P c_p} \left(\frac{e_0 - e_r^*}{T_0 - T_r} \right) + B^{-1} \frac{E_a}{E_0}$$

From this one obtains Penman's expression for the Bowen ratio

$$B = \frac{\gamma}{\Delta} \left(\frac{E_0 - E_a}{E_0} \right) \tag{12.24}$$

where

$$\gamma = \frac{c_p P}{0.622 L_e} \tag{12.25}$$

is the psychrometer constant whose value is about 0.66 mbar K^{-1} at $T = 273$ K and $P = 1000$ mbar and

$$\Delta = (e_0 - e_r^*)/(T_0 - T_r) \cong de_s/dT \tag{12.26}$$

is the slope of the saturated vapor pressure versus temperature curve at $(T_r + T_0)/2$. The crucial approximation in Equation (12.26), originally suggested by Penman (1948), could be justified only when the surface is wet, so that the water vapor pressure e_0 is close to its saturation value at the surface temperature T_0, and the measurement height above the surface is low.

After substituting from Equation (12.24) into Equation (2.3), we obtain the well-known Penman (1948) formula

$$E_0 = \frac{\Delta}{\Delta + \gamma}\left(\frac{R_N - H_G}{L_e}\right) + \frac{\gamma}{\Delta + \gamma} E_a \tag{12.27}$$

It is clear from the above derivation that Penman's formula has a sound theoretical and physical basis, although some investigators have considered it only empirical. In order to determine the evaporation rate from Equation (12.27), one needs measurements or estimates of net radiation and soil heat flux at ground level, together with the measurements of wind speed, temperature, and humidity at a low level (usually 2 m) above the surface. The observational procedure is simplified by the ingenuous way in which the surface temperature has been eliminated from the final result.

Several further simplifications of Penman's approach to determining potential evaporation have been suggested in the literature. For example, over a water surface or a wet land surface the air might be close to saturation in water vapor, so that E_a would be expected to be negligibly small in comparison to E_0. Then, the simplified relation

$$E_0 = \frac{\Delta}{\Delta + \gamma}\left(\frac{R_N - H_G}{L_e}\right) \tag{12.28}$$

should be adequate for determining the potential evaporation or evapotranspiration. The above formula was first suggested by Slatyer and McIlroy (1961), who called the above estimate 'equilibrium evapotranspiration.' It has been observed that the simpler formula [Equation (12.28)] is valid over a wide range of meteorological conditions and even for less than fully saturated surfaces with vegetation. Note that the only meteorological observation required is that of

mean temperature at a low height of about 2 m, in addition to the measurement or estimate of $R_N - H_G$.

When Equation (12.28) is valid, the Bowen ratio is simply estimated as

$$B \cong \gamma/\Delta \tag{12.29}$$

which also follows from Equation (12.24) when $E_a \ll E_0$. Equation (12.29) can be used in conjunction with Equation (12.28) to obtain the sensible heat flux as

$$H_0 \cong [\gamma/(\Delta + \gamma)](R_N - H_G) \tag{12.30}$$

Equations (12.28) and (12.30) are most suitable for determining the surface fluxes of water vapor and heat from routine micrometeorological measurements. Their applicability is, however, limited to wet, bare surfaces and vegetative surfaces with wet foliage over which evapotranspiration is near its potential rate and both H_0 and E_0 are positive (upward) fluxes. For water surfaces and those with tall vegetation, the use of the surface energy balance equation [Equation (2.1)] may not be appropriate. For these, the energy budget for a layer can be used instead, and Equations (12.16), (12.27), (12.28), and (12.30) can be modified accordingly (replacing $R_N - H_G$ with $R_N - H_G - \Delta H_s$).

12.4.6 Gradient or aerodynamic method

This is similar to the gradient method of determining surface heat flux described in Chapter 11. It requires measurements of specific humidity, in addition to those of wind speed and temperature, at two levels in the surface layer. Under neutral stability conditions, both the wind speed and specific humidity follow similar logarithmic profile laws. It is easy to show that the evaporation rate is given by the Thornthwaite–Holtzman formula

$$E_0 = -\rho k^2 \Delta U \Delta Q / [\ln(z_2/z_1)]^2 \tag{12.31}$$

For the more general stratified conditions, following the same procedure as in the determination of momentum and heat fluxes in Chapter 11, the water vapor flux is given by

$$E_0 = -\rho k^2 \Delta U \Delta Q / \phi_m(\zeta_m)\phi_w(\zeta_m)[\ln(z_2/z_1)]^2 \tag{12.32}$$

which may be considered as a generalization of Equation (12.31). Alternatively, one can use the gradient-transport relation [Equation (12.2)] with $K_w = K_H$. The eddy diffusivity may be specified on the basis of Monin–Obukhov similarity relations, as described in Chapter 11.

12.4.7 Profile method

Again, this is similar to the profile method of determining momentum and heat fluxes. The additional profile relationship to be fitted through the specific humidity data is

$$Q = (q_*/k)[\ln z - \psi_w(z/L)] + [Q_0 - (q_*/k)\ln z_0] \tag{12.33}$$

which suggests a plot of Q versus $\ln z - \psi_w(z/L)$ for determining q_* and, if desired, Q_0. The friction velocity u_* is determined from a similar plot of wind profile and, then, the rate of evaporation $E_0 = -\rho u_* q_*$.

Wind, temperature, and specific humidity profiles over bare land and vegetated surface can easily be measured using small masts and portable towers. But, similar profile measurements over the open ocean are made extremely difficult by undesirable motions of any floating platforms and distortion of the air flow around them. Even more difficult to take and interpret are observations in the lowest layer of direct wave influence. Accurate profile measurements in the fully developed region of the atmospheric surface layer have been made from shallow-water towers and platforms, as well as from specially designed stable buoys and research vessels (Paulson *et al.*, 1972). These are found to be consistent and in good agreement with the Monin–Obukhov similarity relations [Equations (11.9)–(11.14)], provided the buoyancy effects of water vapor are included in the definitions of the M–O stability parameter, as described in Section 12.2. For example, Figures 12.5 and 12.6 show average profiles for different stability classes ranging from slightly stable (I) to moderately unstable (V), taken during the 1964 International Indian Ocean Expedition (IIOE). Note that according to the M–O similarity relations [Equation (11.12)], plots of U versus $\ln z - \psi_m$ and Θ versus $\ln z - \psi_h$ are expected to be linear and are shown to be so. Also note the much smaller gradients of wind and temperature over the ocean, compared to those over land surfaces, which limit the accuracy of flux determinations from mean profile measurements.

Example Problem 2

In addition to the wind, temperature, and humidity observations at 10.9 m, given in Example Problem 1, the following measurements were made at a lower height of 2.42 m:

Mean wind speed = 7.33 m s^{-1}.
Mean temperature = 27.55°C.
Mean specific humidity = 16.72 g kg^{-1}.

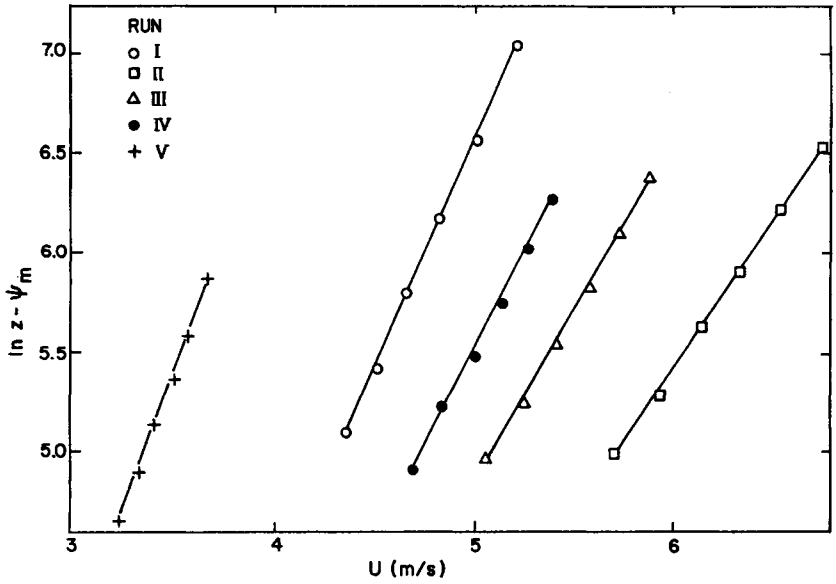

Figure 12.5 Composite wind speeds as functions of $\ln z - \psi_m$ for different stability classes (I–V) during HOE. [After Paulson (1967).]

Use the measurements at the two height levels with the gradient method for estimating the near-surface fluxes of momentum, heat, and water vapor and compare them with those from the bulk-transfer approach used in Example Problem 1.

Solution

Here, $z_1 = 2.42$ m, $z_2 = 10.90$ m, so that

$$z_m = (2.42 \times 10.9)^{1/2} \cong 5.136 \text{ m}$$
$$z_m \ln(z_2/z_1) \cong 7.73 \text{ m}$$

In order to determine the Richardson number at z_m, we calculate the virtual temperatures at the two heights:

$$T_{v1} = 300.70(1 + 0.61 \times 0.01672) \cong 303.77 \text{ K}$$
$$T_{v2} = 300.49(1 + 0.61 \times 0.01604) \cong 304.43 \text{ K}$$

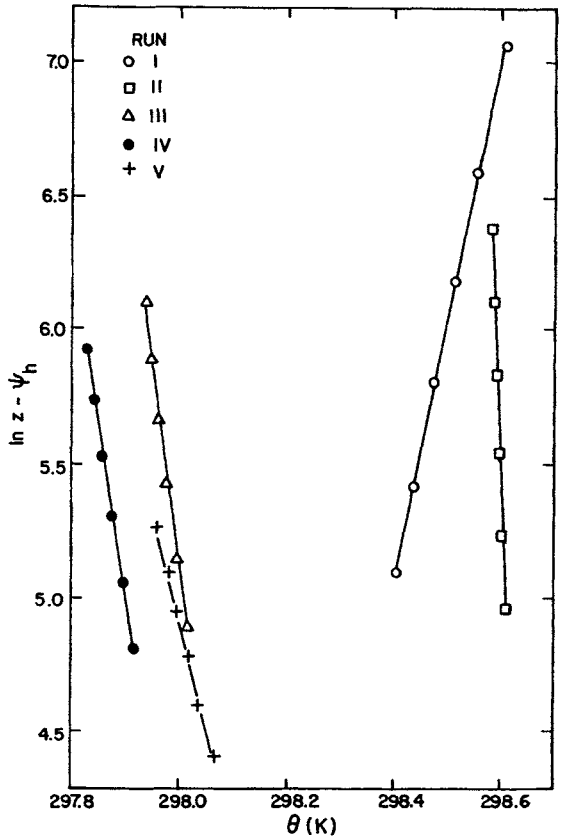

Figure 12.6 Composite potential temperatures as functions of $\ln z - \psi_h$ for different stability classes (I–V) during HOE. [After Paulson (1967).]

Then, using Equation (11.23),

$$\frac{\partial T_v}{\partial z} = \frac{T_{v2} - T_{v1}}{z_m \ln(z_2/z_1)} = -\frac{0.66}{7.73} \cong -0.0854 \text{ K m}^{-1}$$

$$\frac{\partial \Theta_v}{\partial z} = \frac{\partial T_v}{\partial z} + \Gamma = -0.0854 + 0.0098 = -0.0756 \text{ K m}^{-1}$$

$$\frac{\partial U}{\partial z} = \frac{7.96 - 7.33}{7.73} \cong 0.0815 \text{ s}^{-1}$$

$$\text{Ri}_m = -\frac{9.81 \times 0.0756}{304.1 \times (0.0815)^2} \cong -0.367$$

Using Equation (11.25), the M–O stability parameter can be estimated as

$$\zeta_m = \mathrm{Ri}_m \cong -0.367$$

and the corresponding M–O similarity functions are estimated as

$$\phi_m = (1 - 15\zeta_m)^{-1/4} \cong 0.626$$
$$\phi_h = \phi_w = (1 - 15\zeta_m)^{-1/2} \cong 0.392$$

Then, from Equation (11.26), we obtain

$$u_* = \frac{0.4(7.96 - 7.33)}{0.626 \times 1.505} \cong 0.268 \text{ m s}^{-1}$$

$$\theta_* = \frac{0.4(300.60 - 300.72)}{0.392 \times 1.505} \cong -0.0814 \text{ K}$$

$$q_* = \frac{0.4(0.01604 - 0.01672)}{0.392 \times 1.505} \cong -4.61 \times 10^{-4}$$

Using the previously estimated value of $\rho = 1.14$ kg m^{-3}, the surface stress and other fluxes can be determined as

$$\tau_0 = \rho u_*^2 = 1.14 \times (0.268)^2 \cong 0.082 \text{ N m}^{-2}$$
$$H_0 = \rho c_p u_* \theta_* = -1.14 \times 1004 \times 0.268 \times 0.0814 \cong 24.97 \text{ W m}^{-2}$$
$$E_0 = -\rho u_* q_* = 1.14 \times 0.268 \times 4.61 \times 10^{-4} \cong 1.41 \times 10^{-4} \text{ kg m}^{-2} \text{ s}^{-1}$$

These may be compared with the earlier estimated values from the bulk-transfer approach:

$$\tau_0 \cong 0.108 \text{ N m}^{-2}; \; H_0 \cong 12.3 \text{ W m}^{-2}; \; E_0 \cong 0.92 \times 10^{-4} \text{ kg m}^{-2} \text{ s}^{-1}$$

The largest discrepancy between the two methods is found in the determination of the sensible heat flux, presumably due to the large uncertainty in the measurement of the rather small temperature gradient. The given sea-surface temperature may also be in error, because it actually represents the bucket water temperature, rather than the skin surface temperature. The two estimates of the rate of evaporation also differ by 40%, while the discrepancy in the surface stress is about 27%. These differences are consistent with the generally estimated uncertainties of $\pm 20\%$ in estimates of surface fluxes using the various micrometeorological methods.

12.5 Applications

The material presented in this chapter may have the following practical applications:

- Estimating evaporation or evapotranspiration over various types of surfaces.
- Parameterizing the transfer of water vapor to the atmosphere in large-scale atmospheric models.
- Systematic ordering of specific humidity observations in the atmospheric surface layer.
- Determining the water budget of the earth's surface.
- Incorporating the buoyancy effects of water vapor in flux-profile relations in the lower atmosphere.

Problems and Exercises

1.

(a) Considering the flow of moisture only in the vertical direction through a uniform and homogeneous subsurface stratum, derive Equation (12.7) for the soil moisture content.

(b) Describe a plausible method of estimating the rate of evaporation from a bare soil surface, using measurements of the soil moisture content in the topmost layer.

2.

(a) Derive an expression for the virtual heat flux in terms of the sensible and latent heat fluxes.

(b) If evaporation is taking place from a sea surface of temperature 27°C, which is slightly cooler than the air at 10 m height, what value of the Bowen ratio would correspond to the neutral stability? What would be the corresponding heat flux if the rate of evaporation is 2 mm day^{-1}?

3.

(a) If the normalized potential temperature and specific humidity gradients in the surface layer are equal [i.e., $(kz/\theta_*)(\partial\Theta/\partial z) = (kz/q_*)(\partial Q/\partial z)$], show that the eddy diffusivities of heat and water vapor must also be equal (i.e., $K_h = K_w$).

(b) How would you expect the ratio K_w/K_m to vary with stability? Express this ratio as a function of Ri.

(c) Calculate and compare the values of eddy diffusivity K_h or K_w during the typical daytime unstable conditions ($u_* = 0.5$ m s^{-1}, $H_{v0} = 500$ W m^{-2})

and nighttime stable conditions ($u_* = 0.1$ m s^{-1}, $H_{v0} = -50$ W m^{-2}) at a height of 10 m over a bare soil surface.

4. Starting from the instantaneous vertical flux of water vapor, derive the eddy correlation formula for the rate of evaporation $E_0 = \rho\overline{wq}$, and state all the assumptions you have to make.

5. Compare and contrast the energy balance/Bowen ratio method with the bulk transfer method for estimating heat and water vapor fluxes over (a) a short grass surface and (b) an ocean surface. Which method would you recommend in each case?

6. The following micrometeorological measurements of mean wind speed, temperature, specific humidity, and the surface energy budget were made on October 7, 1967, 1200 PST, on a large grass field near Davis, California:

z (m)	U (m s^{-1})	T (°C)	Q (g kg^{-1})
0.25	1.11	23.52	8.22
0.50	1.34	23.35	7.73
1.00	1.51	23.30	6.88
2.00	1.63	23.14	6.65
6.00	1.80	22.95	6.05

Net radiation flux = 450 W m^{-2}
Ground heat flux = 43 W m^{-2}
Average grass height = 0.07 m

(a) Determine the average value of the Bowen ratio.
(b) Calculate the sensible heat flux and the evaporation rate, using the surface energy balance/Bowen ratio method.
(c) Calculate the potential evapotranspiration from the grass surface using the simplified Penman formula [Equation (12.28)] with the observed air temperature at 2 m.
(d) Do the same, but using the original Penman formula [Equation (12.27)] and taking the neutral value of $C_W = C_D = k^2/(\ln z/z_0)^2$.

7. Given the profile data of Problem 6, calculate the sensible heat flux and the rate of evaporation using the following methods:
(a) The gradient or aerodynamic method with observations at heights of 0.5 m and 2 m.
(b) The profile method.